PHOTONICS Research

Room temperature synthesis of stable silica-coated $CsPbBr_3$ quantum dots for amplified spontaneous emission

Qionghua Mo,[1,†] Tongchao Shi,[2,†] Wensi Cai,[1] Shuangyi Zhao,[1,*] Dongdong Yan,[1] Juan Du,[2,3,4] and Zhigang Zang[1,5]

[1]Key Laboratory of Optoelectronic Technology & Systems (Ministry of Education), Chongqing University, Chongqing 400044, China
[2]State Key Laboratory of High Field Laser Physics, Shanghai Institute of Optics and Fine Mechanics, Chinese Academy of Sciences, Shanghai 201800, China
[3]Hangzhou Institute for Advanced Study, University of Chinese Academy of Sciences, Hangzhou 310024, China
[4]e-mail: dujuan@mail.siom.ac.cn
[5]e-mail: zangzg@cqu.edu.cn
*Corresponding author: shyzhao@cqu.edu.cn

Received 10 June 2020; accepted 3 August 2020; posted 10 August 2020 (Doc. ID 399845); published 22 September 2020

All-inorganic cesium lead bromide ($CsPbBr_3$) perovskite quantum dots (QDs) with excellent optical properties have been regarded as good gain materials for amplified spontaneous emission (ASE). However, the poor stability as the results of the high sensitivity to heat and moisture limits their further applications. Here, we report a facile one-pot approach to synthesize $CsPbBr_3$@SiO_2 QDs at room temperature. Due to the effective defects passivation using SiO_2, as-prepared $CsPbBr_3$@SiO_2 QDs present an enhanced photoluminescence quantum yield (PLQY) and chemical stability. The PLQY of $CsPbBr_3$@SiO_2 QDs reaches 71.6% which is higher than 46% in pure $CsPbBr_3$ QDs. The PL intensity of $CsPbBr_3$@SiO_2 QDs maintains 84% while remaining 24% in pure $CsPbBr_3$ after 80 min heating at 60°C. The ASE performance of the films is also studied under a two-photon-pumped laser. Compared with the films using pure $CsPbBr_3$ QDs, those with as-prepared $CsPbBr_3$@SiO_2 QDs exhibit a reduced threshold of ASE. The work suggests that room-temperature-synthesized SiO_2-coated perovskites QDs are promising candidates for laser devices.

https://doi.org/10.1364/PRJ.399845

1. INTRODUCTION

Owing to the outstanding optoelectronic properties, such as high photoluminescence quantum yield (PLQY), flexible tunability of emission wavelength, and narrow emission spectrum, all-inorganic $CsPbX_3$ (X = Cl, Br, I) quantum dots (QDs) have received attentions as promising candidates for the next generation optoelectronic devices [1–3]. The outstanding optical properties make them potentially suitable for using in light-emitting diodes (LEDs) [4–6], solar cells [7,8], photodetectors [9,10], and most importantly as optical gain materials [11–14]. Lasers and amplified spontaneous emission (ASE) from perovskite QDs have been reported recently [15–17]. Yakunin *et al.* first reported the ASE performance of $CsPbBr_3$ QDs under a single-photon-pumped laser [18]. Pan *et al.* showed the ASE threshold of $CsPbBr_3$ QDs film to be 192 μJ/cm^2 and 12 mJ/cm^2 under single-photon and two-photon pumped laser, respectively [19]. Most recently, Song *et al.* embedded $CsPbBr_3$ QDs into an Au@SiO_2 core–shell nanostructure and showed a reduced threshold of 5 mJ/cm^2 under one-photon exciton [20]. In addition, a number of studies were performed to reduce the threshold of ASE and laser [21–24]. However, their practical applications are still limited owing to the poor stability resulting from the high sensitivity to moisture and heat [25–27].

Therefore, various strategies, including coating, doping/alloying heteroatoms, and ligand modification have been studied to improve the stability of $CsPbBr_3$ QDs [28–33]. Our group reported a ligand modification method to synthesize $CsPbBr_3$ QDs by using 2-hexyldecanoic acid (DA), resulting in an excellent stability [34]. Nag *et al.* reported a doping method by using Mn and Yb with a reduced-defect density and enhanced stability [35]. However, ligand modification and elemental doping are not effectively protecting QDs from humidity and heat. Among all these methods, coating is an effective and practical strategy to control the stability and suppress the nonradiative auger recombination [36–39]. Chen *et al.* reported a two-photon-pumped ASE performance by embedding the $CsPbBr_3$ QDs with dual-mesoporous silica [40].

Tang *et al.* showed that by capping $CsPbBr_3$ QDs core with a CdS shell, the chemical stability and two-photon-pumped ASE performance could be improved [41]. Zhang *et al.* embedded $CsPbBr_3$ QDs into silica by tetraethyl orthosilicate (TEOS) hydrolysis, which improved the moisture resistance and enhanced the stability [42]. However, such methods are generally complicated because it requires the use of extra gases during the synthesis and is not time efficient. The high processing temperature and prolonged stirring might also impede further research of stable and efficient gain materials. Therefore, it is quite urgent to exploit a room-temperature synthesis technique, which could synthesize $CsPbBr_3$ QDs with high PLQY and high stability for ASE.

In this work, we synthesized the $CsPbBr_3$ QDs with a high thermal stability by a facile one-step at room temperature method. The QD films were coated with SiO_2 by adding 3-aminopropyl-triethoxysilane (APTES). The PLQY of $CsPbBr_3@SiO_2$ QDs reached 71.6%, while it was only 46% in those with pure $CsPbBr_3$ QDs. In addition, the $CsPbBr_3@SiO_2$ QDs exhibited an excellent stability under heat. An enhanced two-photon pumped ASE that operated in an ambient air condition was also demonstrated. Compared with those using $CsPbBr_3$ QDs, the ASE threshold of $CsPbBr_3@SiO_2$ QDs films was reduced by 70 $\mu J/cm^2$ under a two-photon pumped laser excitation. Such a simple and yet effective method to coat shell onto $CsPbBr_3$ QDs might have potential applications in fields such as room-temperature-operated frequency up-conversion lasers.

2. EXPERIMENT

Chemicals and reagents: $PbBr_2$ (99.99%) and CsBr (99.9%) were purchased from Xi'an Polymer Light Technology Corp. DMF (99.9%, Sigma-Aldrich). OA (90%), OAm (80%–90%), toluene (99.5%), and APTES (99.5%) were obtained from Adamas. All these reagents were used without further purification.

Synthesis of $CsPbBr_3$ QDs: $PbBr_2$ (0.4 mmol) and CsBr (0.4 mmol) were first added in 10 mL of DMF and stirred for 1 h to obtain a clear solution. Then OA (0.6 mL) and OAm (0.2 mL) were added into the precursor solution followed by a stirring for another 30 min. After that, 0.5 mL of the precursor solution was quickly added in a beaker containing 10 mL of toluene under vigorous stirring at 1500 r/min for 10 s.

Synthesis of $CsPbBr_3@SiO_2$ QDs: 0.5 mL precursor solution was quickly added into 10 mL toluene containing 0.69 μL APTES under vigorous stirring at 1500 r/min for 10 s. All the above experiments were carried out at room temperature.

Characterizations: The X-ray diffraction (XRD) characterization was performed using XRD-6100 (Shimadzu, Japan). Fourier transform infrared (FTIR) spectra of the samples were recorded with a Nicolet iS50 (Thermo Fisher Scientific, Waltham, MA, USA). X-ray photoelectron spectroscopy (XPS) profiles were measured on an ESCA Lab220I-XL. The transmission electron microscopy (TEM) was performed using an electron microscope (Libra 200 FE, Zeiss, Germany). Absorption spectrum was enforced by a UV-2100 (Shimadzu, Japan). The photoluminescence spectrum was obtained by a fluorescence spectrophotometer (Agilent Cary Eclipse, Australia) equipped with a Xe lamp. Time-resolved fluorescence spectra were recorded with a GL-3300 (Photon Technology International Inc., USA). The PLQY was investigated by an FLSP920 (Edinburgh Instruments Ltd., UK). The ASE measurements were performed using a pumping source of a Ti:sapphire amplifier system (wavelength: 800 nm, repetition rate: 1 kHz, pulse-width: 50 fs, Solstice, Spectra-Physics). The ASE was detected by a fiber spectrometer (Ocean Optics) with a spectral resolution of 1 nm.

3. RESULTS AND DISCUSSION

$CsPbBr_3@SiO_2$ QDs were obtained through a modified supersaturated recrystallization method at room temperature, and the whole process only took 10 s. As shown in Fig. 1, first CsBr, $PbBr_2$, OA, and OAm (OA:OAm = 3:1, volume ratio) were all mixed in N, N-dimethylformamide (DMF). Precursors were then rapidly injected into the toluene solution, which contained a certain amount of 3-aminopropyl-triethoxysilane (APTES). Upon the injection into a poor solvent of toluene, $CsPbBr_3$ QDs were formed immediately. Meanwhile, APTES gradually linked to the surface of QDs and then reacted with the trace of water from open air to hydrolysis [42]. Finally, silica (SiO_2) was formed and coated onto the $CsPbBr_3$ QDs.

The crystal structure of $CsPbBr_3$ QDs was first studied using X-ray diffraction. As shown in Fig. 2(a), black and red lines

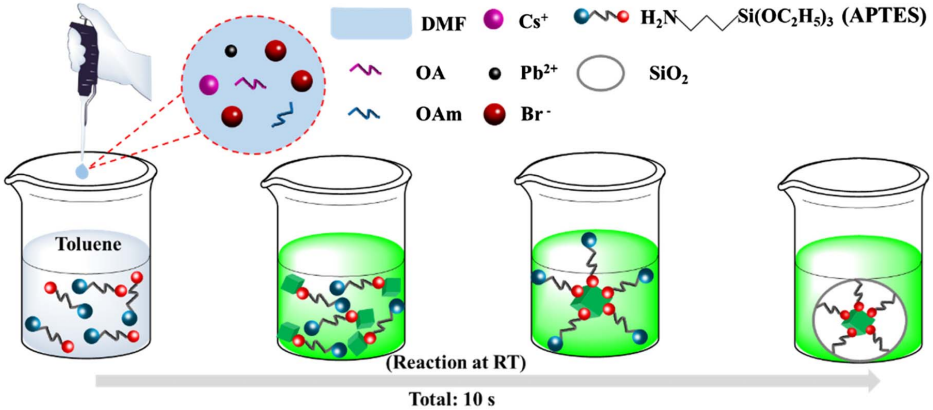

Fig. 1. Reaction process schematics of the formation of $CsPbBr_3@SiO_2$ QDs.

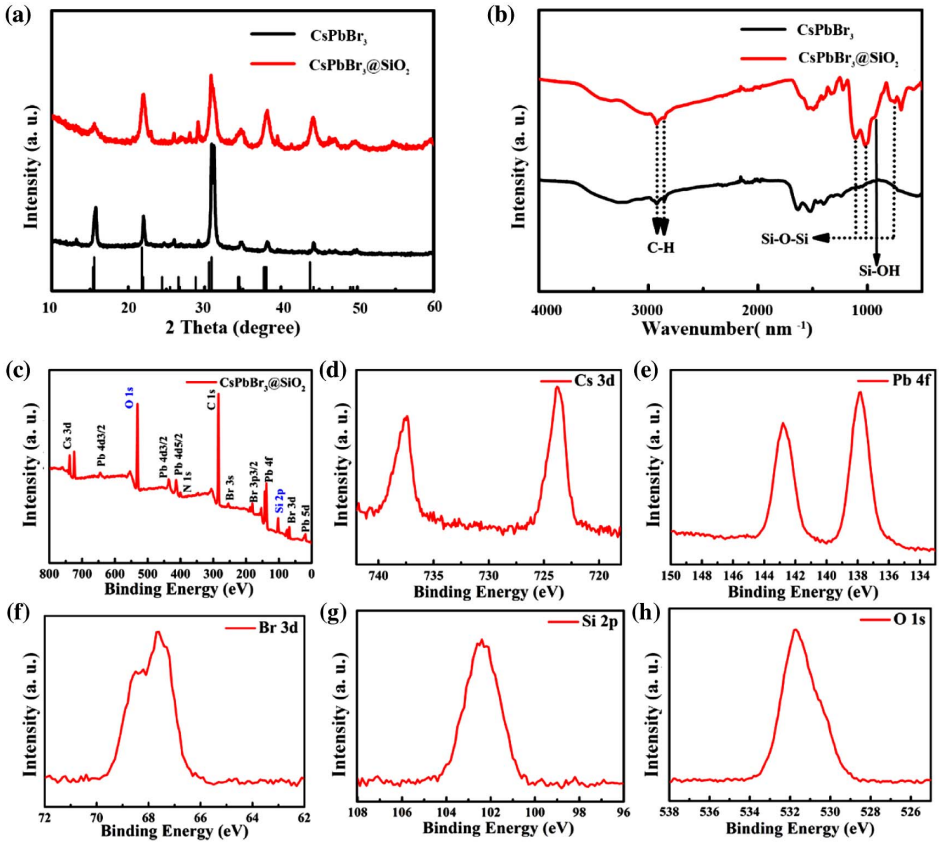

Fig. 2. (a) XRD patterns, (b) FTIR spectra, (c) XPS full scan of $CsPbBr_3@SiO_2$ QDs and the high-resolution XPS profiles of (d) Cs 3d, (e) Pb 4f, (f) Br 3d, (g) Si 2p, and (h) O 1s.

correspond to $CsPbBr_3$ and $CsPbBr_3@SiO_2$ QDs, respectively. The $CsPbBr_3$ QDs exhibit diffraction peaks at 15.66°, 21.96°, 31.01°, 34.87°, 38.15°, and 44.30°, which correspond to the (100), (110), (200), (210), (211), and (202) planes of $CsPbBr_3$ QDs (JCPDS 18-0364), respectively. The XRD patterns of $CsPbBr_3@SiO_2$ are in good agreement with those of $CsPbBr_3$ QDs, indicating that the *in situ* growth of the SiO_2 does not affect the cubic crystal structure of $CsPbBr_3$. Surface functional groups were then determined using Fourier transform infrared spectra of $CsPbBr_3$ and $CsPbBr_3@SiO_2$ QDs shown in Fig. 2(b). While the weak peaks located at 1113, 1013, and 751 cm^{-1} indicate the presence of Si–O–Si bonds, the one located at 925 cm^{-1} corresponds to the existence of Si–OH bonds, both suggesting the presence of SiO_2 in $CsPbBr_3@SiO_2$ QDs. To determine the chemical composition of $CsPbBr_3@SiO_2$ QDs, X-ray photoelectron spectroscopy was also carried out with Fig. 2(c) showing the full scan of $CsPbBr_3@SiO_2$ QDs. While the peaks of Cs 3d [737.5 and 723.8 eV, Fig. 2(d)], Pb 4f [142.8 and 137.9 eV, Fig. 2(e)], and Br 3d [68 eV, Fig. 2(f)] clearly demonstrate the formation of $CsPbBr_3$ [43,44], Si 2p peak [102.4 eV, Fig. 2(g)] and O 1s peak [531.7 eV, Fig. 2(h)] suggest the formation of Si–O–Si bonds [45] and are in agreement with the results obtained from FTIR spectra.

Figures 3(a)–3(d) show the transmission electron microscopy (TEM) and high resolution TEM (HRTEM) images of the obtained $CsPbBr_3$ QDs and $CsPbBr_3@SiO_2$ QDs, respectively. It is found that the $CsPbBr_3@SiO_2$ QDs maintain an orthorhombic morphology, a good dispersity, and the same lattice plane distance of 0.58 nm as pure $CsPbBr_3$ QDs, indicating that the SiO_2 coating has no effect on the crystal structure of $CsPbBr_3$. In addition, it was found that $CsPbBr_3$ QDs were all dispersed and embedded inside the SiO_2. The average size of $CsPbBr_3$ QDs is 13.4 nm [inset of Fig. 3(a)], while a shrinking and narrow size distribution with an average QD size of 12.3 nm is observed in $CsPbBr_3@SiO_2$ QDs [inset of Fig. 3(c)]. This phenomenon might be due to the hydrolysis of APTES, which in turn leads to the presence of silica around the lead ions and binds the growth of perovskite crystals [46]. Figure 3(e) shows the energy-dispersive spectroscopy (EDS) mapping images of $CsPbBr_3@SiO_2$ QDs, from which a uniform distribution of the Cs, Pb, and Br components, and the presence of SiO_2 were observed in the films with $CsPbBr_3@SiO_2$.

As shown in Fig. 4(a), although both $CsPbBr_3$ and $CsPbBr_3@SiO_2$ QDs show green emission colors, the luminescence of $CsPbBr_3@SiO_2$ QDs is greener. In Fig. 4(b), we show the PL emission spectra of both $CsPbBr_3$ QD films with the same quantity, which were measured under the same condition. The PL intensity of the films with $CsPbBr_3@SiO_2$ QDs is almost doubled compared with those using $CsPbBr_3$ QDs. In particular, the PLQY of $CsPbBr_3@SiO_2$ QDs is as high as 71.6%, while it is only 46% in the $CsPbBr_3$ case. As shown

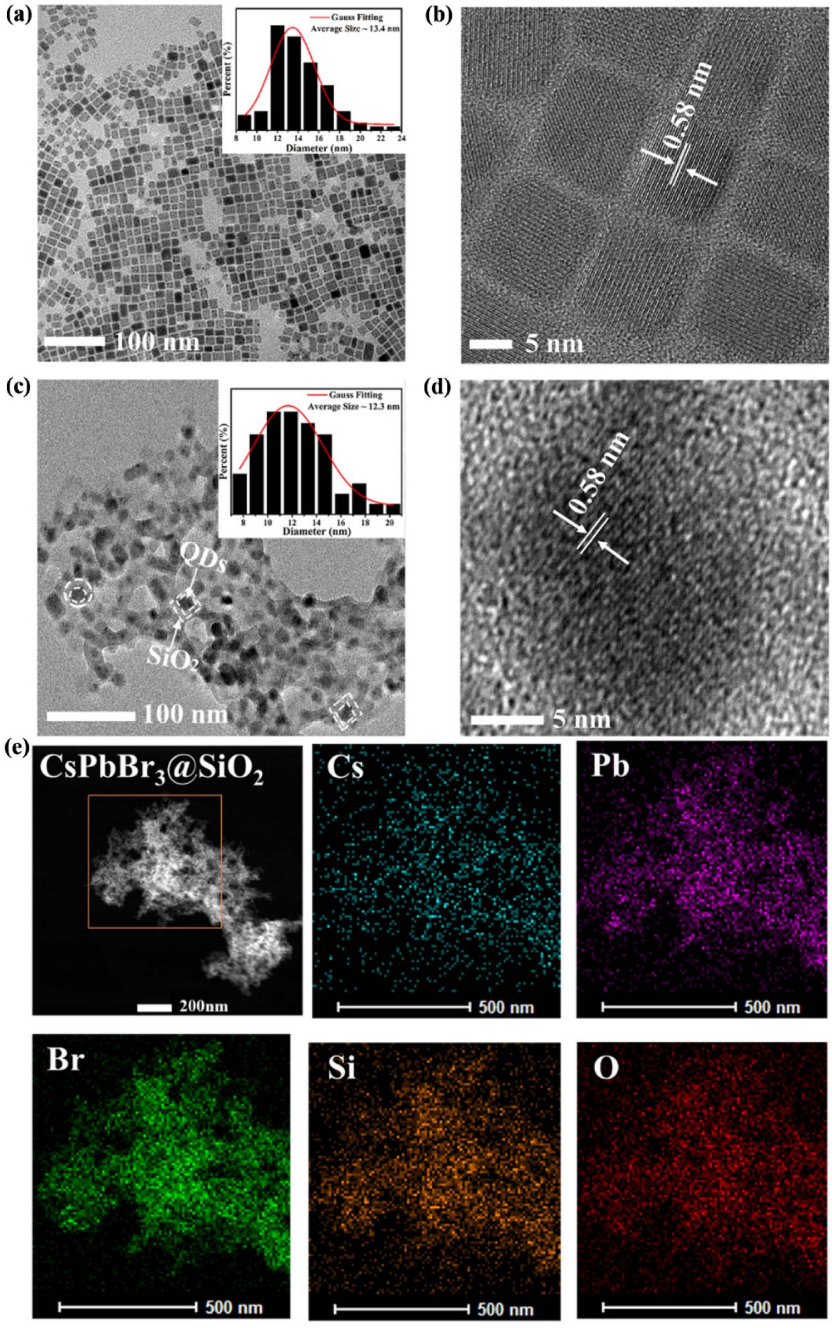

Fig. 3. (a), (c) TEM images and (b), (d) HRTEM images of pure $CsPbBr_3$ and $CsPbBr_3@SiO_2$ QDs. (e) Element distribution of $CsPbBr_3@SiO_2$ QDs.

in Fig. 4(c), the absorption and PL peaks of $CsPbBr_3$ and $CsPbBr_3@SiO_2$ QDs are located at 529/526 nm and 517/508 nm, respectively. For $CsPbBr_3@SiO_2$ QDs films, a blue shift is observed both in the absorption and PL results, which might be due to the decreased QDs size [47]. To understand the carrier dynamics, a PL lifetime measurement was carried out with the results shown in Fig. 4(d). These PL decay curves are fitted with a biexponential function consisting of a fast-decay component (τ_1) and a slow-decay component (τ_2) [48]. The fast-decay component (τ_1) is speculated to be the trap-assisted nonradiative recombination, while the slow-decay component (τ_2) is speculated to be the free-charge carrier radiative recombination [49]. Clearly, the $CsPbBr_3@SiO_2$ QDs exhibit a longer decay time [7.6 ns (τ_1) and 36.6 ns (τ_2)] than $CsPbBr_3$ QDs [4.9 ns (τ_1) and 22.5 ns (τ_2)] [in inset of Fig. 4(d)]. SiO_2 might reduce the surface defect/trap state density of the perovskite QDs, resulting in a suppression of the defect-assisted nonradiative recombination [45]. Therefore, it is believed that such an enhanced PLQY and elongated PL lifetime of $CsPbBr_3@SiO_2$ QDs are mainly due to the passivation effects of SiO_2, and the decrease of the surface defects could contribute to the improvement of the QDs luminescent performance.

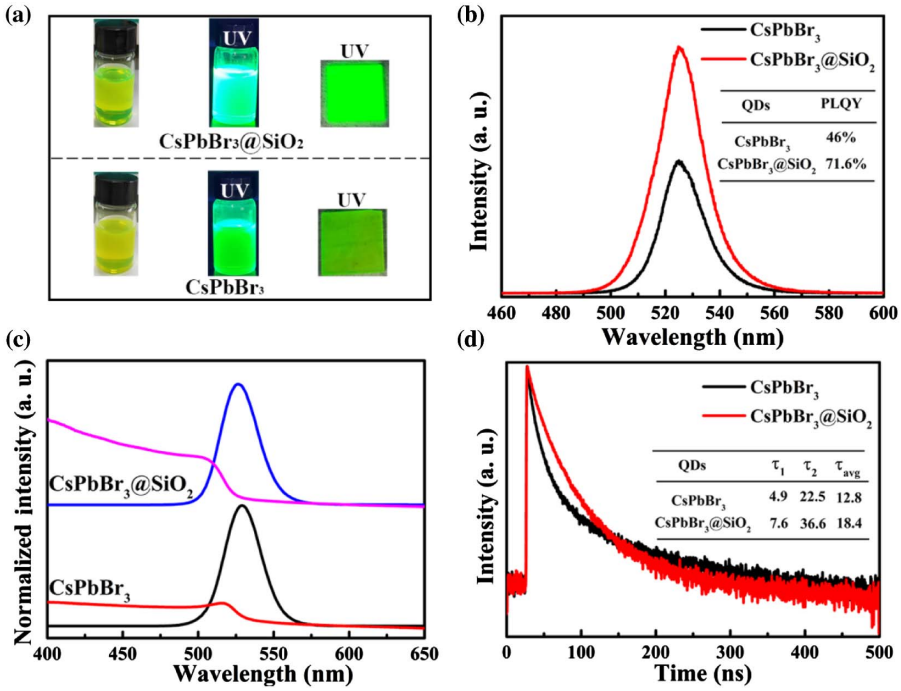

Fig. 4. (a) Photographs of $CsPbBr_3$ and $CsPbBr_3@SiO_2$ QDs solution with/without UV light and films with UV light. (b) PL intensity, (c) Absorption and PL spectra, and (d) PL decay curves of $CsPbBr_3$ and $CsPbBr_3@SiO_2$ QDs.

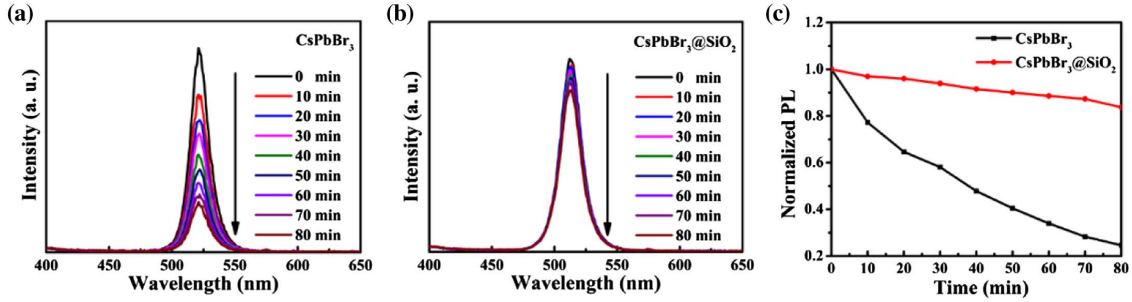

Fig. 5. PL spectra of (a) $CsPbBr_3$ and (b) $CsPbBr_3@SiO_2$. (c) Normalized PL intensity of $CsPbBr_3$ and $CsPbBr_3@SiO_2$ under continuous heating at 60°C.

Subsequently, the thermal effects on the PL performance of $CsPbBr_3$ and $CsPbBr_3@SiO_2$ QDs films were tested, as shown in Fig. 5. While the PL intensity of $CsPbBr_3$ QDs film decreases quickly under the heating at 60°C [Fig. 5(a)], the $CsPbBr_3@SiO_2$ QDs film exhibits a slow decrease in PL intensity [Fig. 5(b)]. Although both types of the films show a decrease of PL intensity over time, the films with $CsPbBr_3@SiO_2$ QDs maintain 84% of their initial PL intensity, while only 24% remains in the case with pure $CsPbBr_3$ after 80 min continuous heating, indicating that the $CsPbBr_3@SiO_2$ QDs film is fairly resistant to heat and possesses a good chemical stability. This result confirms that coating the $CsPbBr_3$ QDs film with SiO_2 could significantly enhance the thermal stability of perovskite, which is critical for optoelectronics in future practical applications.

All-inorganic $CsPbX_3$ perovskites were previously reported to exhibit excellent potentials as candidates for lasers and two-photon-excited up-conversion devices [50,51]. To further study the potential of our materials, $CsPbBr_3$ and $CsPbBr_3@SiO_2$ QDs were deposited on glass to obtain ASE performance under a two-photon (800 nm) excitation at room temperature. At a relatively low pump excitation, a broad spontaneous emission (SE) with a peak centered at 529 nm and an FWHM of 23 nm are found for $CsPbBr_3$ QDs film, as shown in Fig. 6(a). With the increase of pump density, a peak located at 535 nm emerges and quickly becomes dominant. Meanwhile, the FWHM of the emission spectra narrows sharply to 4.9 nm [Fig. 6(b)], suggesting the transition from SE to ASE regimes. As shown in Fig. 6(c), the emission of $CsPbBr_3@SiO_2$ QDs films has similar features: initially a broad SE shows at low pump and quickly transforms to an obvious ASE phenomenon with the increase of pump output power [Fig. 6(c)]. Also, the FWHM of the emission spectra narrows sharply from 25 to 3 nm, as shown in Fig. 6(d).

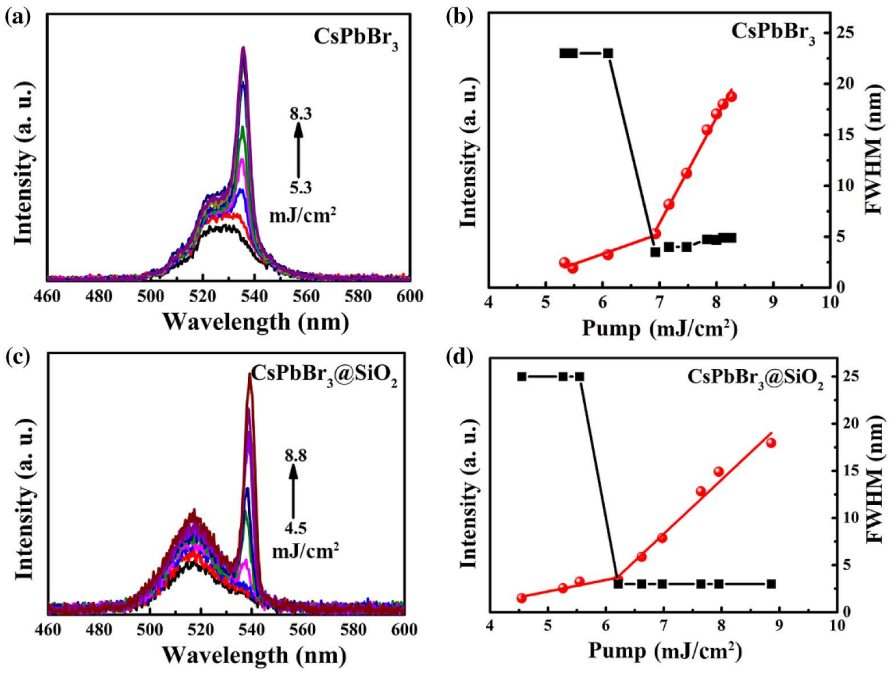

Fig. 6. (a) Pump-intensity dependence of the emission from the $CsPbBr_3$ film under an 800 nm femtosecond laser excitation. (b) Output intensity (red) and linewidth (black) as functions of pump energy density for $CsPbBr_3$ film under a femtosecond laser excitation of 800 nm. (c) Pump-intensity dependence of the emission from the $CsPbBr_3@SiO_2$ film under an 800 nm femtosecond laser excitation. (d) Output intensity (red) and linewidth (black) as functions of pump energy density for $CsPbBr_3@SiO_2$ film under a femtosecond laser excitation of 800 nm.

The thresholds (P_{th}) of two-photon pumped ASE are found to be about 6.9 and 6.2 mJ/cm^2 for $CsPbBr_3$ QDs and $CsPbBr_3@SiO_2$ QDs films, respectively, under excitation of 800 nm and 35 fs laser pulses. A clear decrease of ASE threshold for 70 $\mu J/cm^2$ is found here owing to the effective capping with SiO_2, suggesting such a method is promising for depositing laser devices.

4. CONCLUSION

$CsPbBr_3@SiO_2$ QDs were synthesized by a one-step *in situ* method at room temperature in air. By coating with SiO_2, surface defects of $CsPbBr_3$ QDs are passivated, which suppresses the defect-assisted nonradiative recombination. As a result, the PLQY of $CsPbBr_3$ QDs increases from 46% to 71.6%, and the thermal stability significantly improves. In addition, under the two-photon (800 nm) pump laser excitations, the ASE threshold of $CsPbBr_3@SiO_2$ QDs film is 70 $\mu J/cm^2$ lower than that of the $CsPbBr_3$ QDs film owing to the effective SiO_2 passivation. The results demonstrate a simple synthesis method to coat SiO_2 with $CsPbBr_3$ QDs at room temperature, which also provides an industry-compatible deposition method for lasers.

Funding. National Natural Science Foundation of China (61875211, 61904023, 61905264, 61925507, 11974063); Fundamental Research Funds for the Central Universities (2019CDJGFGD001); National Key Research and Development Program of China (2017YFE0123700); Strategic Priority Research Program of CAS (XDB16030400); CAS Interdisciplinary Innovation Team, Program of Shanghai Academic/Technology Research Leader (18XD1404200).

Disclosures. The authors declare that there are no conflicts of interest related to this paper.

†These authors contributed equally to this work.

REFERENCES

1. X. Li, Y. Wang, H. Sun, and H. Zeng, "Amino-mediated anchoring perovskite quantum dots for stable and low-threshold random lasing," Adv. Mater. **29**, 1701185 (2017).
2. X. Li, Y. Wu, S. Zhang, B. Cai, Y. Gu, J. Song, and H. Zeng, "$CsPbX_3$ quantum dots for lighting and displays: room-temperature synthesis, photoluminescence superiorities, underlying origins and white light-emitting diodes," Adv. Funct. Mater. **26**, 2435–2445 (2016).
3. L. Protesescu, S. Yakunin, M. I. Bodnarchuk, F. Krieg, R. Caputo, C. H. Hendon, R. X. Yang, A. Walsh, and M. V. Kovalenko, "Nanocrystals of cesium lead halide perovskites ($CsPbX_3$, X = Cl, Br, and I): novel optoelectronic materials showing bright emission with wide color gamut," Nano Lett. **15**, 3692–3696 (2015).
4. J. Liu, J. Zhou, H. Lin, Y. Yu, S. Zuo, and B. Li, "Bright luminous and stable $CsPbBr_3$@PS microspheres prepared via facile anti-solvent method using CTAB as double modifier," Chem. Eur. J. **26**, 10528–10533 (2020).
5. Y.-H. Suh, T. Kim, J. W. Choi, C.-L. Lee, and J. Park, "High-performance $CsPbX_3$ perovskite quantum-dot light-emitting devices via solid-state ligand exchange," ACS Appl. Nano Mater. **1**, 488–496 (2018).
6. J. H. Park, A. Y. Lee, J. C. Yu, Y. S. Nam, Y. Choi, J. Park, and M. H. Song, "Surface ligand engineering for efficient perovskite

nanocrystal-based light-emitting diodes," ACS Appl. Mater. Interfaces **11**, 8428–8435 (2019).
7. X. Yang, H. Yang, X. Hu, W. Li, Z. Fang, K. Zhang, R. Huang, J. Li, Z. Yang, and Y. Song, "Low-temperature interfacial engineering for flexible $CsPbI_2Br$ perovskite solar cells with high performance beyond 15%," J. Mater. Chem. A **8**, 5308–5314 (2020).
8. M. B. Faheem, B. Khan, C. Feng, M. U. Farooq, F. Raziq, Y. Xiao, and Y. Li, "All-inorganic perovskite solar cells: energetics, key challenges, and strategies toward commercialization," ACS Energy Lett. **5**. 290–320 (2019).
9. P. Ramasamy, D. H. Lim, B. Kim, S. H. Lee, M. S. Lee, and J. S. Lee, "All-inorganic cesium lead halide perovskite nanocrystals for photodetector applications," Chem. Commun. **52**, 2067–2070 (2016).
10. L. Lv, Y. Xu, H. Fang, W. Luo, F. Xu, L. Liu, B. Wang, X. Zhang, D. Yang, W. Hu, and A. Dong, "Generalized colloidal synthesis of high-quality, two-dimensional cesium lead halide perovskite nanosheets and their applications in photodetectors," Nanoscale **8**, 13589–13596 (2016).
11. H. Zhang, M. Jin, X. Liu, Y. Zhang, Y. Yu, X. Liang, W. Xiang, and T. Wang, "The preparation and up-conversion properties of full spectrum $CsPbX_3$ (X = Cl, Br, I) quantum dot glasses," Nanoscale **11**, 18009–18014 (2019).
12. X. Li, W. Liu, Y. Song, H. Long, K. Wang, B. Wang, and P. Lu, "Two-photon-pumped high-quality, single-mode vertical cavity lasing based on perovskite monocrystalline films," Nano Energy **68**, 104334 (2020).
13. Y. Liu, Z. Gao, W. Zhang, X. Sun, Z. Wang, X. Wang, B. Xu, and X. Meng, "Stimulated emission from $CsPbBr_3$ quantum dot nanoglass," Opt. Mater. Express **9**, 3390–3405 (2019).
14. Y. Yang, Q. Li, Y. Liu, R. Cong, Y. Sun, J. Hou, M. Ge, J. Shi, F. Zhang, G. Zhao, N. Zhang, Y. Fang, and N. Dai, "Magenta-emitting cesium lead halide nanocrystals encapsulated in dimethicone for white light-emitting diodes," ACS Appl. Nano Mater. **3**, 4886–4892 (2020).
15. J. Chen, K. Zidek, P. Chabera, D. Liu, P. Cheng, L. Nuuttila, M. J. Al-Marri, H. Lehtivuori, M. E. Messing, K. Han, K. Zheng, and T. Pullerits, "Size- and wavelength-dependent two-photon absorption cross section of $CsPbBr_3$ perovskite quantum dots," J. Phys. Chem. Lett. **8**, 2316–2321 (2017).
16. M. L. De Giorgi, F. Krieg, M. V. Kovalenko, and M. Anni, "Amplified spontaneous emission threshold reduction and operational stability improvement in $CsPbBr_3$ nanocrystals films by hydrophobic functionalization of the substrate," Sci. Rep. **9**, 17964 (2019).
17. X. Wu, Y. Li, W. Li, L. Wu, B. Fu, W. Wang, G. Liu, D. Zhang, J. Zhao, and P. Chen, "Enhancing optically pumped organic-inorganic hybrid perovskite amplified spontaneous emission via compound surface plasmon resonance," Crystals **8**, 124 (2018).
18. S. Yakunin, L. Protesescu, F. Krieg, M. I. Bodnarchuk, G. Nedelcu, M. Humer, G. De Luca, M. Fiebig, W. Heiss, and M. V. Kovalenko, "Low-threshold amplified spontaneous emission and lasing from colloidal nanocrystals of cesium lead halide perovskites," Nat. Commun. **6**, 8056 (2015).
19. J. Pan, S. P. Sarmah, B. Murali, I. Dursun, W. Peng, M. R. Parida, J. Liu, L. Sinatra, N. Alyami, C. Zhao, E. Alarousu, T. K. Ng, B. S. Ooi, O. M. Bakr, and O. F. Mohammed, "Air-stable surface-passivated perovskite quantum dots for ultra-robust, single- and two-photon-induced amplified spontaneous emission," J. Phys. Chem. Lett. **6**, 5027–5033 (2015).
20. L. Zhao, Y. Chen, X. Yu, X. Xing, J. Chen, J. Song, and J. Qu, "Low-threshold stimulated emission in perovskite quantum dots: single-exciton optical gain induced by surface plasmon polaritons at room temperature," J. Mater. Chem. C **8**, 5847–5855 (2020).
21. Y. Wang, X. Li, X. Zhao, L. Xiao, H. Zeng, and H. Sun, "Nonlinear absorption and low-threshold multiphoton pumped stimulated emission from all-inorganic perovskite nanocrystals," Nano Lett. **16**, 448–453 (2016).
22. Y. Wang, M. Zhi, Y. Q. Chang, J. P. Zhang, and Y. Chan, "Stable, ultralow threshold amplified spontaneous emission from $CsPbBr_3$ nanoparticles exhibiting trion gain," Nano Lett. **18**, 4976–4984 (2018).
23. L. Wang, L. Meng, L. Chen, S. Huang, X. Wu, G. Dai, L. Deng, J. Han, B. Zou, C. Zhang, and H. Zhong, "Ultralow-threshold and color-tunable continuous-wave lasing at room temperature from *in situ* fabricated perovskite quantum dots," J. Phys. Chem. Lett. **10**, 3248–3253 (2019).
24. X. Tang, Y. Bian, Z. Liu, J. Du, M. Li, Z. Hu, J. Yang, W. Chen, and L. Sun, "Room-temperature up-conversion random lasing from $CsPbBr_3$ quantum dots with TiO_2 nanotubes," Opt. Lett. **44**, 4706–4709 (2019).
25. A. Mikosch, S. Ciftci, G. Tainter, R. Shivanna, B. Haehnle, F. Deschler, and A. J. C. Kuehne, "Laser emission from self-assembled colloidal crystals of conjugated polymer particles in a metal-halide perovskite matrix," Chem. Mater. **31**, 2590–2596 (2019).
26. S. Yuan, D. Chen, X. Li, J. Zhong, and X. Xu, "*In situ* crystallization synthesis of $CsPbBr_3$ perovskite quantum dot-embedded glasses with improved stability for solid-state lighting and random upconverted lasing," ACS Appl. Mater. Interfaces **10**, 18918–18926 (2018).
27. H. Zhang, L. Yuan, Y. Chen, Y. Zhang, Y. Yu, X. Liang, W. Xiang, and T. Wang, "Amplified spontaneous emission and random lasing using $CsPbBr_3$ quantum dot glass through controlling crystallization," Chem. Commun. **56**, 2853–2856 (2020).
28. S. Wang, J. Yu, M. Zhang, D. Chen, C. Li, R. Chen, G. Jia, A. L. Rogach, and X. Yang, "Stable, strongly emitting cesium lead bromide perovskite nanorods with high optical gain enabled by an intermediate monomer reservoir synthetic strategy," Nano Lett. **19**, 6315–6322 (2019).
29. Z.-J. Li, E. Hofman, J. Li, A. H. Davis, C.-H. Tung, L.-Z. Wu, and W. Zheng, "Photoelectrochemically active and environmentally stable $CsPbBr_3/TiO_2$ core/shell nanocrystals," Adv. Funct. Mater. **28**, 1704288 (2018).
30. X. Liu, X. Zhang, L. Li, J. Xu, S. Yu, X. Gong, J. Zhang, and H. Yin, "Stable luminescence of $CsPbBr_3$/*n*CdS core/shell perovskite quantum dots with Al self-passivation layer modification," ACS Appl. Mater. Interfaces **11**, 40923–40931 (2019).
31. H. C. Wang, S. Y. Lin, A. C. Tang, B. P. Singh, H. C. Tong, C. Y. Chen, Y. C. Lee, T. L. Tsai, and R. S. Liu, "Mesoporous silica particles integrated with all-inorganic $CsPbBr_3$ perovskite quantum-dot nanocomposites (MP-PQDs) with high stability and wide color gamut used for backlight display," Angew. Chem. **55**, 7924–7929 (2016).
32. T. Xuan, X. Yang, S. Lou, J. Huang, Y. Liu, J. Yu, H. Li, K. L. Wong, C. Wang, and J. Wang, "Highly stable $CsPbBr_3$ quantum dots coated with alkyl phosphate for white light-emitting diodes," Nanoscale **9**, 15286–15290 (2017).
33. J. Zhu, Z. Xie, X. Sun, S. Zhang, G. Pan, Y. Zhu, B. Dong, X. Bai, H. Zhang, and H. Song, "Highly efficient and stable inorganic perovskite quantum dots by embedding into a polymer matrix," Chem. Nano Mater. **5**, 346–351 (2018).
34. D. Yan, T. Shi, Z. Zang, T. Zhou, Z. Liu, Z. Zhang, J. Du, Y. Leng, and X. Tang, "Ultrastable $CsPbBr_3$ perovskite quantum dots and their enhanced amplified spontaneous emission by surface ligand modification," Small **15**, 1901173 (2019).
35. W. J. Mir, Y. Mahor, A. Lohar, M. Jagadeeswararao, S. Das, S. Mahamuni, and A. Nag, "Postsynthesis doping of Mn and Yb into $CsPbX_3$ (X = Cl, Br, or I) perovskite nanocrystals for down-conversion emission," Chem. Mater. **30**, 8170–8178 (2018).
36. S. Lou, Z. Zhou, T. Xuan, H. Li, J. Jiao, H. Zhang, R. Gautier, and J. Wang, "Chemical transformation of lead halide perovskite into insoluble, less cytotoxic, and brightly luminescent $CsPbBr_3/CsPb_2Br_5$ composite nanocrystals for cell imaging," ACS Appl. Mater. Interfaces **11**, 24241–24246 (2019).
37. S. Huang, Z. Li, L. Kong, N. Zhu, A. Shan, and L. Li, "Enhancing the stability of $CH_3NH_3PbBr_3$ quantum dots by embedding in silica spheres derived from tetramethyl orthosilicate in 'waterless' toluene," J. Am. Chem. Soc. **138**, 5749–5752 (2016).
38. Y. Wei, K. Li, Z. Cheng, M. Liu, H. Xiao, P. Dang, S. Liang, Z. Wu, H. Lian, and J. Lin, "Epitaxial growth of $CsPbX_3$ (X = Cl, Br, I) perovskite quantum dots via surface chemical conversion of Cs_2GeF_6 double perovskites: a novel strategy for the formation of leadless hybrid perovskite phosphors with enhanced stability," Adv. Mater. **31**, 1807592 (2019).
39. B. Wang, C. Zhang, S. Huang, Z. Li, L. Kong, L. Jin, J. Wang, K. Wu, and L. Li, "Postsynthesis phase transformation for $CsPbBr_3/Rb_4PbBr_6$ core/shell nanocrystals with exceptional photostability," ACS Appl. Mater. Interfaces. **10**, 23303–23310 (2018).

40. Y. Chen, M. Yu, S. Ye, J. Song, and J. Qu, "All-inorganic $CsPbBr_3$ perovskite quantum dots embedded in dual-mesoporous silica with moisture resistance for two-photon-pumped plasmonic nanolasers," Nanoscale **10**, 6704–6711 (2018).
41. X. Tang, J. Yang, S. Li, Z. Liu, Z. Hu, J. Hao, J. Du, Y. Leng, H. Qin, X. Lin, Y. Lin, Y. Tian, M. Zhou, and Q. Xiong, "Single halide perovskite/semiconductor core/shell quantum dots with ultrastability and nonblinking properties," Adv. Sci. **6**, 1900412 (2019).
42. Q. Zhong, M. Cao, H. Hu, D. Yang, M. Chen, P. Li, L. Wu, and Q. Zhang, "One-pot synthesis of highly stable $CsPbBr_3@SiO_2$ core-shell nanoparticles," ACS Nano **12**, 8579–8587 (2018).
43. B. Qiao, P. Song, J. Cao, S. Zhao, Z. Shen, G. Di, Z. Liang, Z. Xu, D. Song, and X. Xu, "Water-resistant, monodispersed and stably luminescent $CsPbBr_3/CsPb_2Br_5$ core-shell-like structure lead halide perovskite nanocrystals," Nanotechnology **28**, 445602 (2017).
44. S. Fang, G. Li, H. Li, Y. Lu, and L. Li, "Organic titanates: a model for activating rapid room-temperature synthesis of shape-controlled $CsPbBr_3$ nanocrystals and their derivatives," Chem. Commun. **54**, 3863–3866 (2018).
45. C. Sun, Y. Zhang, C. Ruan, C. Yin, X. Wang, Y. Wang, and W. W. Yu, "Efficient and stable white LEDs with silica-coated inorganic perovskite quantum dots," Adv. Mater. **28**, 10088–10094 (2016).
46. Z. Liu, Y. Zhang, Y. Fan, Z. Chen, Z. Tang, J. Zhao, Y. Lv, J. Lin, X. Guo, J. Zhang, and X. Liu, "Toward highly luminescent and stabilized silica-coated perovskite quantum dots through simply mixing and stirring under room temperature in air," ACS Appl. Mater. Interfaces **10**, 13053–13061 (2018).
47. W. Chen, J. Hao, W. Hu, Z. Zang, X. Tang, L. Fang, T. Niu, and M. Zhou, "Enhanced stability and tunable photoluminescence in perovskite $CsPbX_3/ZnS$ quantum dot heterostructure," Small **13**, 1604085 (2017).
48. N. Yarita, H. Tahara, T. Ihara, T. Kawawaki, R. Sato, M. Saruyama, T. Teranishi, and Y. Kanemitsu, "Dynamics of charged excitons and biexcitons in $CsPbBr_3$ perovskite nanocrystals revealed by femtosecond transient-absorption and single-dot luminescence spectroscopy," J. Phys. Chem. Lett. **8**, 1413–1418 (2017).
49. Y. Rakita, N. Kedem, S. Gupta, A. Sadhanala, V. Kalchenko, M. L. Böhm, M. Kulbak, R. H. Friend, D. Cahen, and G. Hodes, "Low-temperature solution-grown $CsPbBr_3$ single crystals and their characterization," Cryst. Growth Des. **16**, 5717–5725 (2016).
50. X. Tang, Z. Hu, W. Yuan, W. Hu, H. Shao, D. Han, J. Zheng, J. Hao, Z. Zang, J. Du, Y. Leng, L. Fang, and M. Zhou, "Perovskite $CsPb_2Br_5$ microplate laser with enhanced stability and tunable properties," Adv. Opt. Mater. **5**, 1600788 (2017).
51. S. Liu, X. Fang, Y. Wang, and X. Zhang, "Two-photon pumped amplified spontaneous emission based on all-inorganic perovskite nanocrystals embedded with gold nanorods," Opt. Mater. **81**, 55–58 (2018).